PAPER

Check for updates

PDEGMA-*b*-PDMAEMA-*b*-PLMA triblock terpolymers and their cationic analogues: synthesis, stimuli responsive self-assembly and micelleplex formation†

Despoina Giaouzi and Stergios Pispas [ID] *

In this study, the synthesis, chemical modification and self-assembly in aqueous media of novel temperature-responsive and pH-responsive triblock terpolymers of the type (poly(diethylene glycol methyl ether methacrylate)-*b*-poly(2-(dimethylamino)ethyl methacrylate)-*b*-poly(lauryl methacrylate)) (PDEGMA-*b*-PDMAEMA-*b*-PLMA) are reported. The triblock terpolymers were synthesized *via* RAFT polymerization and molecular characterization was achieved by SEC, ^{1}H-NMR and FTIR spectroscopy. Methyl iodide (CH$_3$I) was utilized for chemical modification of the PDMAEMA blocks to increase the overall solubility of the triblock terpolymers in aqueous media and to obtain permanent positive charges, converting them to temperature-responsive block polyelectrolytes. PDEGMA-*b*-PDMAEMA-*b*-PLMA triblock terpolymers and their quaternized analogs self-assemble in aqueous media forming spherical micellar structures consisting of a hydrophobic PLMA core and stimuli-responsive PDMAEMA and PDEGMA corona, as evidenced by light scattering measurements. The dimensions of the formed micelles were influenced noticeably by variations in the solution temperature and pH. Moreover, we examine the formation of micelleplexes between quaternized PDEGMA-*b*-QPDMAEMA-*b*-PLMA thermoresponsive micelles and DNA molecules. The complexation capability of the formed micelleplexes was investigated by ethidium bromide quenching assays utilizing fluorescence spectroscopy techniques and UV-vis spectroscopy. Light scattering techniques are utilized in order to determine the structural characteristics of the formed micelleplexes. The quaternized terpolymer micelles effectively interact with nucleic acid molecules with their surface charge and their size depending on the composition of block terpolymers, the N/P ratio, and the increase of temperature above the LCST value of the temperature responsive PDEGMA block.

Introduction

Stimuli-responsive polymers are a class of smart materials that have attracted scientific interest due to their ability to form nanoscale structures of diverse morphologies in aqueous media.[1,2] This property renders them useful as nanocarriers for triggered and targeted delivery of therapeutic and bioimaging molecules and genes. Stimuli-responsive polymers are capable of self-assembling in aqueous media in response to one or more external stimuli[1–3] such as temperature,[4] pH,[5,6] and ionic strength[7,8] and undergoing variations, irreversible or reversible, in their conformation and physical/chemical pro-

perties. Stimuli-responsive polymers are promising, potential candidates for a wide range of applications in various scientific fields such as medicine, biotechnology and diagnostics.[9,10]

Temperature-responsive polymers, among the most significant subclasses of stimuli-responsive polymers, exhibit abrupt variations in the solvation state after the solution temperature changes.[4,11–13] Temperature-responsive polymers are broadly divided into two main groups. The first comprises polymers that become insoluble/hydrophobic when the temperature rises above a lower critical solution temperature (LCST) and the second one includes polymers that become soluble/hydrophilic when the temperature rises above an upper critical solution temperature (UCST).[13–16] Temperature-responsive polymers are examined in aqueous solutions since they are capable of emulating biological systems and responding to physiological conditions.[4] These kinds of synthetic polymers have attracted enormous scientific attention due to their promising applications in biomedical fields such as gene and drug delivery.[17–22]

Theoretical and Physical Chemistry Institute, National Hellenic Research Foundation, 48 Vassileos Constantinou Avenue, Athens 11635, Greece.
E-mail: pispas@eie.gr
†Electronic supplementary information (ESI) available. See DOI: https://doi.org/10.1039/d4py00144c

Among temperature-responsive polymers, PDEGMA (poly (diethylene glycol methyl ether methacrylate)) is a thermo-responsive, hydrophilic polymer, which becomes hydrophobic above its transition temperature (~27 °C, molar mass dependent).[23,24] Copolymers composed of PDEGMA are promising candidates as nanocarriers/biomaterials for biomedical applications since the PDEGMA polymer presents high biocompatibility.[25]

Another important category of stimuli-responsive polymers includes pH-responsive polymers that undergo alternations in the hydration and conformational state in response to changes in solution pH.[9,26–29] Poly(2-(dimethylamino) ethyl methacrylate) PDMAEMA is a homopolymer that responds to changes in solution pH ($pK_a \approx 7.5$) as well as in solution temperature when pH ≥ 7 exhibiting a transition temperature in the range from 40 °C to 55 °C. The transition temperature of the PDMAEMA homopolymer depends on its molecular weight and the solution pH and ionic strength, which affect the protonation degree of the amine groups and the resulting electrostatic interactions.[30,31] The cationic character of pH-responsive polymers and their pH swelling/deswelling properties make them outstanding candidates as non-viral synthetic nanocarriers in gene therapy.[32–35]

Among nonviral gene vectors, lipids[36–38] and cationic polymers[39,40] have emerged as efficient vectors in gene therapy methodologies. However, the usage of cationic polymers as gene carriers displays some advantages in comparison to the usage of lipids, specifically the increased stability of the polyplexes against nuclease degradation, the formulation of polyplexes with narrow size distributions and relatively small dimensions and the perspective of increasing the payload of the vectors.[41–43] Cationic polymers need to be developed with controlled compositions, molecular weights and architecture, which are parameters of numerous importance in designing and formulating efficient gene delivery systems.

Cationic polymers demonstrate the tendency to form polyplexes after simple mixing with nucleic acid molecules because of the electrostatic interactions developed between the positively charged groups of the cationic polymer and the negatively charged phosphate groups of nucleic acids.

In the present study, our investigation effort concentrated on the synthesis of (poly(diethylene glycol methyl ether methacrylate)-b-poly(2-(dimethylamino)ethyl methacrylate)-b-poly(lauryl methacrylate)) (PDEGMA-b-PDMAEMA-b-PLMA) triblock terpolymers, their molecular characterization, and their chemical modification in order to produce amphiphilic cationic block polyelectrolytes. For the chemical modification of the PDMAEMA block, methyl iodide (CH₃I) is utilized as the quaternizing agent, resulting in PDEGMA-b-QPDMAEMA-b-PLMA quaternized triblock terpolymers. Moreover, we study the self-assembly properties of amino-based and quaternized triblock terpolymers in aqueous media under different physicochemical conditions, concerning temperature and pH, by means of light scattering techniques and fluorescence spectroscopy. Furthermore, we examined the ability of PDEGMA-b-QPDMAEMA-b-PLMA thermoresponsive, cationic micelles to interact with DNA molecules. The leading goal of this part of our study is the physiochemical characterization of the formed PDEGMA-b-QPDMAEMA-b-PLMA/DNA micelleplexes in order to verify the successful complexation and afterward to clarify the parameters that may affect the micelleplex structure and stability at selected temperatures. The DEGMA monomer was chosen because of its temperature-responsive character and its high biocompatibility.[23,24] DMAEMA is a pH-responsive monomer ordinarily integrated into block copolymers and PDMAEMA is utilized in a considerable range of applications, such as gene or drug delivery carriers.[44,45] The LMA monomer was selected due to its strong hydrophobicity that is a consequence of the long hydrocarbon side chain and because of its biocompatibility.[46,47]

Experimental

Materials

Monomers, di(ethylene glycol) methyl ether methacrylate (DEGMA, 95%), 2(dimethylamino)ethyl methacrylate (DMAEMA, 98%) and lauryl methacrylate (LMA, 96%) were purchased from Sigma Aldrich and passed through an inhibitor removing column. AIBN (2,2′-azobis(isobutyronitrile)) was recrystallized in ethanol and further utilized as a solution in dioxane, 4-cyano-4-[(dodecylsulfanylthiocarbonyl)sulfanyl]pentanoic acid (CDTP), methyl iodide (CH₃I), tetrahydrofuran (THF, 99.9%) and linear deoxyribonucleic acid sodium salt from salmon testes with a length of ~113 bp, were purchased from Sigma Aldrich and utilized as obtained. For assays of the polyplex formation, ethidium bromide (EtBr) used as fluorescent DNA intercalating probe and sodium chloride (NaCl, ≥99.0%) utilized for the preparation of 0.01 M and 1 M NaCl solutions were obtained from Sigma Aldrich and utilized as received.

PDEGMA homopolymer synthesis

The PDEGMA homopolymer was synthesized via RAFT polymerization using 4-cyano-4-[(dodecylsulfanylthiocarbonyl) sulfanyl]pentanoic acid (CDTP) as the chain transfer agent (CTA), AIBN as the initiator and 1,4 dioxane as the solvent of the polymerization reaction. DEGMA (3 g, 15.93 mmol), CDTP (0.346 g, 15.93 mmol), AIBN (0.014 g, 0.086 mmol as a solution in 1,4-dioxane) (moles CDTP : moles AIBN = 10 : 1) were dissolved in 1,4-dioxane (15 mL) and the polymerization solution was poured into a round bottom flask (25 mL) equipped with a magnetic stirrer and then air-tightly sealed with a rubber septum. Subsequently, the final polymerization solution was degassed by a continuous flow of high purity nitrogen gas for 15 minutes and placed in a thermostatic oil bath at 70 °C for 6 hours. After termination of the polymerization reaction by placing the flask in a refrigerator at −20 °C for 10 min and exposure to air, macro-CTA PDEGMA was isolated by precipitation in excess n-hexane twice, after intermediate redissolution in THF. Consequently, the product was placed in a vacuum oven to be dried for 48 hours at ambient temperature

and after that period, the PDEGMA homopolymer was collected (yield: 86%) before being used for the polymerization of the DMAEMA monomer. The average molecular weight (M_w) was 3400 g mol^{-1} and the molecular weight dispersity index (M_w/M_n) was 1.19, both values were extracted by size exclusion chromatography (SEC) measurements.

PDEGMA-*b*-PDMAEMA block copolymer synthesis

In order to synthesize PDEGMA-*b*-PDMAEMA block copolymer, PDEGMA was utilized as the macro-CTA, AIBN as the radical initiator and 1,4-dioxane as the polymerization solvent. The synthesis process of the intermediate PDEGMA-*b*-PDMAEMA block copolymer is described as follows: DMAEMA monomer (1 g, 6.36 mmol), PDEGMA macro-CTA (1 g, 0.294 mmol) and AIBN (0.004829 g, 0.0294 mmol) were dissolved in 10 mL of 1,4-dioxane. The polymerization solution was placed in a round bottom flask with a magnetic stirrer and fitted with a rubber septum. After 15 min degassing by bubbling high purity nitrogen gas, the flask was placed in a thermostatic oil bath at 65 °C for 18 hours. The polymerization reaction was terminated by placing the flask in a refrigerator and exposure to air. The isolation of the PDEGMA-*b*-PDMAEMA block copolymer was achieved by precipitation in an excess of *n*-hexane and subsequently the copolymer was placed in a vacuum oven for 48 hours for drying. Then, the block copolymer was collected (yield: 89%). The average molecular weight was M_w = 4300 g mol^{-1} and the molecular weight dispersity index was M_w/M_n = 1.23, as determined by size exclusion chromatography (SEC).

PDEGMA-*b*-PDMAEMA-*b*-PLMA triblock terpolymer synthesis

For the preparation of PDEGMA-*b*-PDMAEMA-*b*-PLMA triblock terpolymers, the PDEGMA-*b*-PDMAEMA diblock copolymer was used as the macro-CTA, 1,4-dioxane as the solvent and AIBN as the radical initiator. For instance, the process for the synthesis of PDEGMA$_{23}$-*b*-PDMAEMA$_{23}$-*b*-PLMA$_8$-1 triblock terpolymer (the subscripts display the monomeric units in each block of the triblock) as follows: LMA monomer (0.3 g, 1.16 mmol), PDEGMA-*b*-PDMAEMA (0.7 g, 0.163 mmol) and AIBN (0.01335 g, 0.08135 mmol) were dissolved in 10 mL of 1,4-dioxane. The polymerization solution was placed in a round bottom flask equipped with a magnetic stirrer and

sealed with a septum. Afterwards, the solution was degassed by passing pure N$_2$ gas for 15 minutes and the flask was placed in an oil bath at 70 °C for 18 hours. After termination of the reaction by cooling the polymerization solution at −20 °C in a refrigerator and by exposure to air, the triblock PDEGMA$_{23}$-*b*-PDMAEMA$_{23}$-*b*-PLMA$_8$-1 was isolated by precipitation in excess of *n*-hexane. Consequently, the triblock terpolymer was dried in a vacuum oven for 48 hours at ambient temperature (yield: 93%). The average molecular weight was M_w = 10 100 g mol^{-1} and the molecular weight dispersity index was M_w/M_n = 1.27, as determined by size exclusion chromatography (SEC). Three triblock terpolymers were prepared having different compositions of the blocks and molecular weights (Table 1).

Quaternization reaction of PDEGMA-*b*-PDMAEMA-*b*-PLMA triblock terpolymers

The conversion of the tertiary amine groups of the PDMAEMA block into cationic quaternary amine groups was achieved *via* a chemical quaternization reaction utilizing methyl iodide (CH$_3$I) as the quaternizing agent. The typical chemical modification procedure followed for the terpolymers is described briefly here: the triblock was dissolved in the THF solvent (2% w/v) in a round bottom flask equipped with a magnetic stirrer. Afterwards, an excess of quaternizing agent (CH$_3$I) was added to the solution (moles CH$_3$I/moles amine = 2). The quaternization reaction took place at room temperature for 24 hours, under stirring. After this period, the THF solvent was evaporated utilizing a rotary evaporator at ambient temperature and the dry triblock terpolymer was collected and placed in a vacuum oven in order to ensure complete drying of the product.

Self-assembly studies of triblock terpolymers in aqueous media

Aqueous stock solutions of PDEGMA-*b*-PDMAEMA-*b*-PLMA triblock terpolymers were prepared by dissolving the appropriate triblock quantity in the THF solvent and then the mixture was injected into distilled water under vigorous stirring. Subsequently, the THF solvent was evaporated using a rotary evaporator at room temperature and the aqueous polymer solutions were allowed to equilibrate overnight. Aqueous solu-

Table 1 Molecular characterization results for all synthesized amino and quaternized triblock terpolymers

Sample	M_w ($\times10^4$)[a] (g mol^{-1})	M_w/M_n[a]	%wt PDEGMA	%wt PDMAEMA	%wt PLMA
PDEGMA	0.34	1.15	—	—	—
PDEGMA-*b*-PDMAEMA	0.43	1.23	52[b]	48[b]	—
PDEGMA$_{23}$-*b*-PDMAEMA$_{23}$-*b*-PLMA$_8$-1	1.10	1.27	43[b]	36[b]	21[b]
PDEGMA$_{17}$-*b*-PDMAEMA$_{14}$-*b*-PLMA$_6$-2	0.70	1.31	46[b]	32[b]	22[b]
PDEGMA$_{15}$-*b*-PDMAEMA$_8$-*b*-PLMA$_3$-3	0.49	1.26	58[b]	27[b]	15[b]
PDEGMA$_{23}$-*b*-QPDMAEMA$_{23}$-*b*-PLMA$_8$-1	1.33[c]	—	32[c]	52[c]	16[c]
PDEGMA$_{17}$-*b*-QPDMAEMA$_{14}$-*b*-PLMA$_6$-2	0.90[c]	—	36[c]	47[c]	17[c]
PDEGMA$_{15}$-*b*-QPDMAEMA$_8$-*b*-PLMA$_3$-3	0.60[c]	—	47[c]	41[c]	12[c]

[a] Determined by SEC in THF/5% v/v triethylamine. [b] Determined by ^{1}H-NMR in CDCl$_3$ for amine triblock terpolymers. [c] M_w is calculated assuming 100% conversion of the quaternization reaction.

tions of PDEGMA-*b*-PDMAEMA-*b*-PLMA were prepared at pH = 3, pH = 7 and pH = 10. The solution pH was adjusted by adding an appropriate quantity of 0.1 M solution of HCl or NaOH before the dissolution of triblock terpolymers. The quaternized triblock terpolymers were prepared at neutral pH by directly dissolving the desired amount of polymer in the appropriate volume of distilled water. The stock solutions were left overnight so as to ensure complete dissolution of quaternized block terpolymers. The concentration of all prepared solutions was 5×10^{-4} g mL^{-1}.

Complexation of PDEGMA-*b*-QPDMAEMA-*b*-PLMA micelles with DNA molecules

Complexes of cationic triblock terpolymers with DNA molecules (~113 bp) were prepared by mixing the cationic polymer solution (5×10^{-4} g m^{-1} L in 0.01 M NaCl) and DNA solution (5×10^{-4} g mL^{-1} in 0.01 M NaCl) under gentle stirring at neutral pH and room temperature. The micelleplexes were prepared at specific N/P ratios (moles of amine group/moles of phosphate group) in the range of 0.5 : 1 to 8 : 1 by adding the appropriate volume of DNA solution into polymer solution under stirring. The polymer concentration remained constant at all N/P ratios, while DNA solution was added in different quantities to accomplish the desired N/P ratio. The final volume of all cationic polymer/DNA solutions was 10 mL. Furthermore, the polymer/DNA solutions were incubated at ambient temperature overnight for the optimum equilibration of micelleplexes.

Characterization methods

The molecular weights and molecular weight distributions of all synthesized polymers were determined by size exclusion chromatography (SEC) utilizing a Waters system, consisting of a Waters 1515 isocratic pump, a set of three μ-Styragel mixed bed columns (porosity range from 102 to 106 Å), a Waters 2414 refractive index detector (at 40 °C) and controlled through Breeze software. Tetrahydrofuran (THF) was the mobile phase (containing 5% v/v triethylamine), at a flow rate of 1 mL min^{-1} and the temperature was set at 30 °C. Linear polystyrene samples having average molecular weights in the range of 1200 to 152 000 g mol^{-1} and narrow molecular weight distributions were utilized as standards to calibrate the setup. The samples were directly dissolved in the mobile phase. The concentrations of the samples were in the range of 2–4 mg ml^{-1}.

The ^{1}H-NMR measurements were recorded on a Bruker AC 300 FT-NMR spectrometer, using deuterated solvent (deuterated chloroform, CDCl$_3$, and water, D$_2$O). Tetramethylsilane (TMS) was utilized as the internal standard and the chemical shifts are given in parts per million (ppm). The NMR spectra were analyzed using MestReNOva software.

PDEGMA$_{17}$-*b*-PDMAEMA$_{14}$-*b*-PLMA$_6$-2 (Fig. 2, 300 MHz, CDCl$_3$, ppm): 4.09 (2H, –COOC*H*$_2$CH$_2$–), 3.67–3.55 (6H, –CO$_2$C*H*$_2$C*H*$_2$OC*H*$_2$CH$_2$–), 3.39 (3H, –OC*H*$_3$), 2.58 (2H, –C*H*$_2$N (CH$_3$)$_2$), 2.30 (3H, –CH$_2$N(C*H*$_3$)$_2$), 1.93–1.87 (2H, –C*H*$_2$O–), 1.70–1.53 (2H, –OCH$_2$(C*H*$_2$)$_{10}$–), 1.27 (2H, –CH$_2$(C*H*$_2$)$_{10}$CH$_3$–), 1.03 (3H, –C*H*$_3$), 1.42 (2H, –C*H*$_2$–), 0.85 (3H, –CH$_2$CC*H*$_3$–).

Fourier transform infrared spectroscopy (FTIR) measurements were conducted on a Fourier transform instrument (Bruker Equinox 55), equipped with a single bounce attenuated total reflectance (ATR) diamond accessory (Dura-Samp1IR II by SensIR Technologies) at ambient temperature in the range of 5000–550 cm^{-1}.

The following ATR-FTIR spectral peaks of PDEGMA-*b*-PDMAEMA-*b*-PLMA were observed: 2935 cm^{-1}, 2860 cm^{-1} and 1455 cm^{-1} (–CH$_2$), 2828 cm^{-1} and 2771 cm^{-1} (–N(CH$_3$)$_2$), 1720 cm^{-1} (C=O), 1149 cm^{-1} (C–N). PDEGMA-*b*-QPDMAEMA-*b*-PLMA: 3450 cm^{-1} and 1630 cm^{-1} (OH), 3010 cm^{-1}, 1474 cm^{-1}, and 950 cm^{-1} (C–N(CH$_3$)$_3$$^+$), 2920 cm^{-1} and 2850 cm^{-1} (CH$_2$), 1720 cm^{-1} (C=O).

Dynamic light scattering (DLS) measurements were carried out on an ALV/CGS-3 compact goniometer system (AVL GmbH, Germany), utilizing an ALV-5000/EPP multi-tau digital correlator with 288 channels and an ALV/LSE-5003 light scattering electronic unit for stepper motor drive and limit switch control. Moreover, a JDS Uniphase 22 mW He–Ne laser (λ = 632.8 nm) was used as the light source. The instrument is equipped with a temperature controlled circulating water bath for controlling the temperature of the cell. The cumulant method and CONTIN algorithm were utilized for the analysis of autocorrelation functions. All solutions were filtered through hydrophilic 0.45 μm PVDF syringe filters (Membrane Solutions) to remove the dust particles before the measurements. Subsequently, the solutions were placed in cylindrical quartz cuvettes and the angular range was 30°–150° for all measurements. The temperature of the measurements was in the range of 25–55 °C, and it was accomplished by gradually elevating solution temperature by steps of 5 °C with 15 min equilibration between different temperatures. Furthermore, the amino-based triblock terpolymers were examined at different solution pH values (pH = 3, 7 and 10). Before the dissolution of triblock terpolymers, the solution pH was adjusted by addition of 0.1 M HCl or NaOH solutions in neutral aqueous media. The solutions of micelleplexes were placed in cylindrical quartz cuvettes and left for 15 minutes in order to equilibrate. The measurements at all N/P ratios were performed at 25 °C and 45 °C (temperature above the LCST value of the thermoresponsive PDEGMA block). Static light scattering (SLS) measurements were performed on the same instrument. The angular range examined was from 30° to 150° and the temperature dependent measurements were conducted in the range from 25 °C to 55 °C. The calibration standard was spectroscopic grade toluene. The dn/dc values for the triblocks were extracted according to the refractive indices of the constituting blocks and that of water, utilizing also the composition of the triblocks as determined by NMR measurements. The static light scattering results were analyzed by using partial Zimm plots. The concentration of all triblock terpolymer solutions was 5×10^{-4} g mL^{-1}.

Electrophoretic light scattering (ELS) measurements were conducted on a Nano Zeta Sizer (Malvern Instruments) equipped with a 4 mW solid-state laser (λ = 633 nm) and the backscattering angle was fixed at 173°. The Henry correction of

Smoluchowski's equation was used for extraction of data, after equilibration at 25 °C and 45 °C. The ζ-potential values were determined as the average of 50 runs.

Ultraviolet-Visible (UV-Vis) spectroscopy measurements on micelleplexes were carried out in the wavelength range from 200 to 400 nm using a Perkin Elmer (Lambda 19) UV–vis-NIR spectrometer (Waltman, MA, USA). The micelleplexes were measured at different N/P ratios in the range from 0.5 : 1 to 8 : 1.

Fluorescence spectroscopy (FS) measurements of ethidium bromide (EtBr) have been recorded in order to examine the capability of the triblock terpolymers to complex with DNA molecules at various N/P ratios. Specifically, initial stock solutions of nucleic acid molecules (1×10^{-4} g ml^{-1}) were prepared in NaCl (0.01 M), followed by the addition of EtBr ([EtBr] = [P]/4). Afterwards, the DNA stock solutions containing appropriate quantities of EtBr were titrated with a concentrated triblock solution in the range of N/P ratios from 0.0 to 8.0. Upon addition of each cationic triblock, the mixed solution was left for 15 minutes to equilibrate before being measured. Fluorescence spectroscopy experiments were carried out using a Fluorolog-3 Jobin Yvon-Spex spectrofluorometer (model GL3-21) and the emission and excitation wavelengths for the measurements were 600 nm and 535 nm, respectively.

The determination of critical micelle concentration (CMC) of the synthesized triblock terpolymers was achieved via fluorescence spectroscopy experiments utilizing pyrene as the fluorescent probe. A stock solution of pyrene (1 mM) in acetone was prepared. For the experiments, 1 μL of pyrene stock solution was added per 1 mL of aqueous polymer solution and subsequently the system was left for 24 hours at ambient temperature in order to achieve the evaporation of acetone. For the measurements, the excitation wavelength was 335 nm and the emission spectra were recorded in the region 355–630 nm. No excimer formation was noticed for the polymer solutions.

Results and discussion

Synthesis and molecular characterization of triblock terpolymers

Three temperature and pH-responsive PDEGMA-*b*-PDMAEMA-*b*-PLMA amphiphilic triblock terpolymers were successfully synthesized having different molecular weights and compositions of the blocks via a three-step sequential RAFT polymerization process as presented in Scheme 1. The used CTA was CDTP since it is known from the literature[48] that it is reactive for methacrylic monomers, producing well-defined polymers with controlled molecular weights and rather symmetrical and narrow molecular weight distributions. The utilization of the specific CTA was found to result in a well-defined PDEGMA homopolymer and PDEGMA-*b*-PDMAEMA diblock copolymer, which are utilized as the precursors for the synthesis of final triblock terpolymers (Table 1).

The tertiary amine groups of the PDMAEMA block were chemically modified to quaternary amine groups via a quaternization reaction using CH$_3$I as a quaternizing agent (Scheme 1b) in order to produce strong cationic polyelectrolytes.

The molecular characterization of all synthesized triblock terpolymers was accomplished by SEC and ^{1}H-NMR measurements and the extracted molecular characterization results are listed in Table 1.

The PDEGMA-*b*-PDMAEMA-*b*-PLMA triblock terpolymers synthesized have narrow, symmetrical molecular weight distributions and well-controlled compositions and molecular weights, which are in accordance with the stoichiometric calculations utilized in the synthetic route (Table 1). The SEC chromatograms of the PDEGMA$_{17}$-*b*-PDMAEMA$_{14}$-*b*-PLMA$_6$-2 triblock terpolymer depicted in Fig. 1 demonstrate the gradual increase in the molecular weight after the formation of each block. The rather symmetric chromatography peaks with a small level of tailing indicate an almost complete reinitiation of each polymerization step and define the extension of the sequence of macromolecular blocks generated. In all cases molecular weight polydispersities are within the range typically reported for RAFT polymerization techniques.[48]

The chemical structures as well as the compositions of the amine-based triblock terpolymers were identified via ^{1}H-NMR spectroscopy in deuterated chloroform (CDCl$_3$). Taking into account the yields of each polymerization step, the composition values calculated from the characteristic peaks of each block are close to the stoichiometrically calculated values, which indicates the controlled character of the synthetic route followed. The representative spectrum of the PDEGMA$_{17}$-*b*-PDMAEMA$_{14}$-*b*-PLMA$_6$-2 triblock terpolymer is shown in Fig. S1.† The characteristic peaks utilized for the determination of composition are the one at 3.64 ppm (k, 3H, –CH$_3$ protons of the oligo ethylene glycol side chain of the PDEGMA block),[49] the one at 2.31 ppm (e, 6H, –CH$_3$ protons of the tertiary amino group of PDMAEMA block)[50,51] and the one at 1.25 ppm (f, 20H, –CH$_2$ protons in the side chain of PLMA block).[52] The molecular weights and compositions of PDEGMA-*b*-QPDMAEMA-*b*-PLMA cationic triblock terpolymers were determined based on the molecular weights and the compositions of the amine-based PDEGMA-*b*-PDMAEMA-*b*-PLMA terpolymers as determined by SEC and as calculated by means of ^{1}H-NMR spectroscopy, respectively. The molecular weights and the composition of cationic triblock terpolymers were calculated considering that the quaternization reaction is almost quantitative and the tertiary amine group is converted to the quaternary amine group at >97% yield.[53] Acid titrations confirmed that the remaining non-quaternized amine groups were less than 5%. Hence, each methyl group (CH$_3$) of the CH$_3$I quaternizing agent will be incorporated into the tertiary amine group of each PDMAEMA unit and iodine as a counter ion. The molecular weight and composition of the PDEGMA-*b*-QPDMAEMA-*b*-PLMA quaternized triblock terpolymer are summarized in Table 1. In addition, the typical yields of the quaternized triblock terpolymers were >97%.
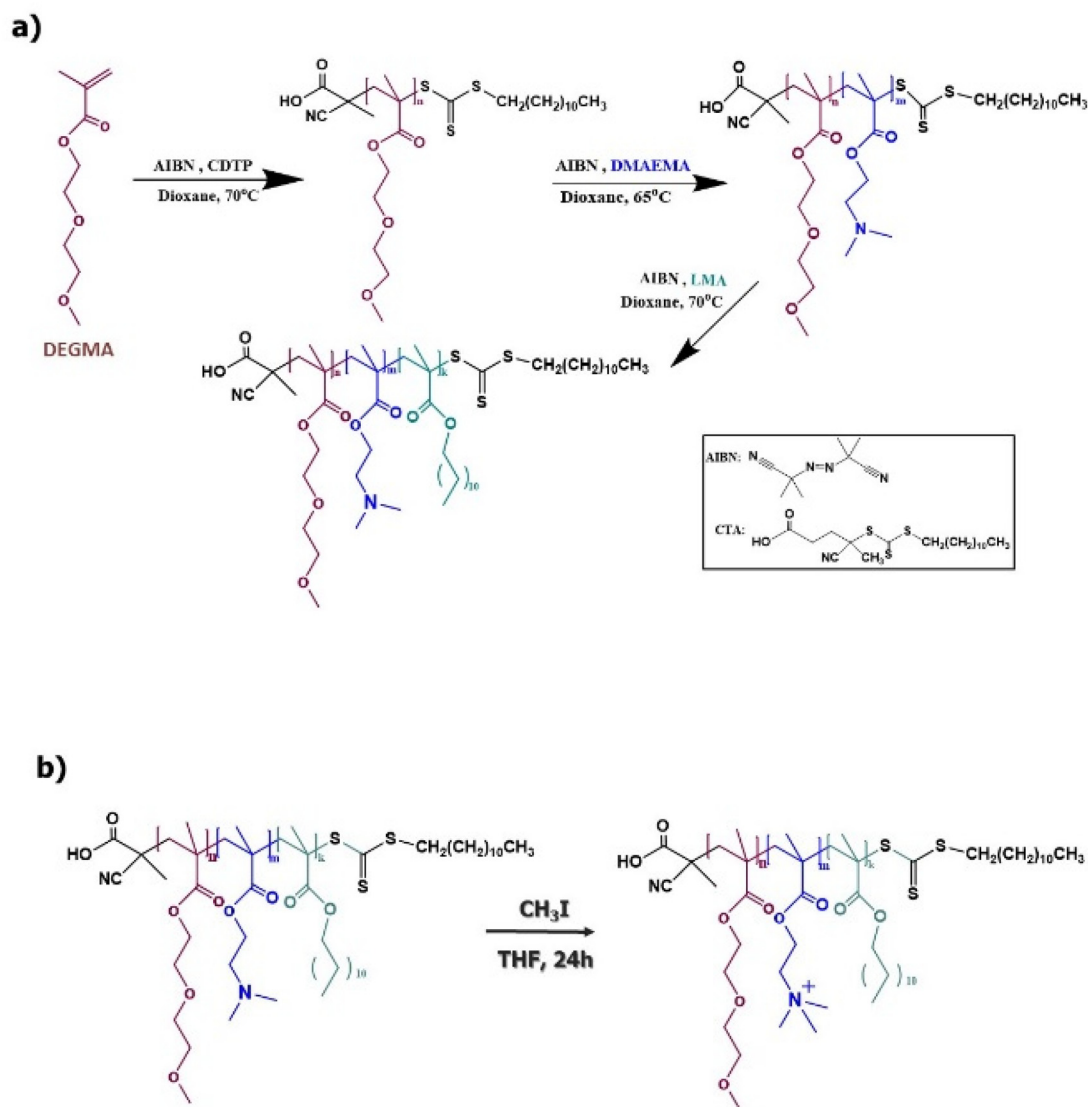
Scheme 1 (a) Synthetic process of PDEGMA-*b*-PDMAEMA-*b*-PLMA triblock terpolymers utilizing RAFT polymerization techniques. (b) Quaternization reaction of the PDEGMA-*b*-PDMAEMA-*b*-PLMA triblock terpolymers.

The conversion of the PDMAEMA tertiary amine group to quaternary ammonium salt was verified by FT-IR spectroscopy. Fig. S2† illustrates the FT-IR spectra of the amine-based PDEGMA$_{17}$-*b*-PDMAEMA$_{14}$-*b*-PLMA$_6$-2 terpolymer and the quaternized PDEGMA$_{17}$-*b*-QPDMAEMA$_{14}$-*b*-PLMA$_6$-2 terpolymer. It can be obviously observed that new absorption peaks appear in the PDEGMA$_{17}$-*b*-QPDMAEMA$_{14}$-*b*-PLMA$_6$-2 spectrum, which are absent in the PDEGMA$_{17}$-*b*-PDMAEMA$_{14}$-*b*-PLMA$_6$-2 spectrum.

The absorption peak at 3448 cm^{-1} corresponds to the stretching of the OH group, as the quaternized product contains some moisture. According to the literature,[54] the peaks at 950 cm^{-1}, 1474 cm^{-1}, and 3005 cm^{-1} are attributed to the C–N (CH)$_3$ stretching of the quaternary amine group. The fingerprint region in FT-IR spectra was the same for all PDEGMA-*b*-QPDMAEMA-*b*-PLMA cationic triblock terpolymers.

Consequently, FT-IR spectroscopy confirmed the successful conversion of PDEGMA-*b*-PDMAEMA-*b*-PLMA amine-based triblock terpolymers to the PDEGMA-*b*-QPDMAEMA-*b*-PLMA cationic polyelectrolytes.

Self-assembly of triblock terpolymers in aqueous media

Taking into consideration the composition, the nature and the sequence of the three blocks, the synthesized PDEGMA-*b*-PDMAEMA-*b*-PLMA amphiphilic terpolymers, as well as their quaternized analogues, are expected to self-assemble into micelles when introduced into aqueous media.[55–57] Moreover, the triblock terpolymers should self-assemble into micelles in aqueous solutions in response to solution pH variations because of the pH-dependent ionization character of the PDMAEMA block and to temperature changes due to the PDEGMA and PDMAEMA blocks. The hydrophobic PLMA
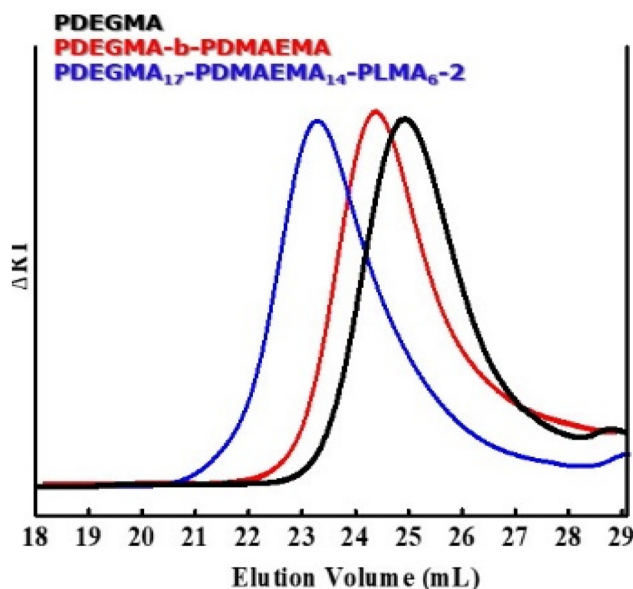
Fig. 1 SEC chromatographs depicting the synthetic sequence for the PDEGMA$_{17}$-b-PDMAEMA$_{14}$-b-PLMA$_6$-2 triblock terpolymer.

block will form the micellar core and the external stimuli-responsive (temperature and pH) blocks PDEGMA and PDMAEMA (or QPDMAEMA) will constitute the mixed corona of the formed micelles where the PDMAEMA block forms the inner part and PDEGMA block constitutes the outer part. A graphical illustration of the self-assembly procedure of PDEGMA-b-PDMAEMA-b-PLMA terpolymers in neutral aqueous medium and at temperatures below and above the LCST values of both PDEGMA and PDMAEMA blocks is presented in Scheme 2.

Dynamic (DLS) and static (SLS) light scattering measurements were performed for all synthesized triblock terpolymers
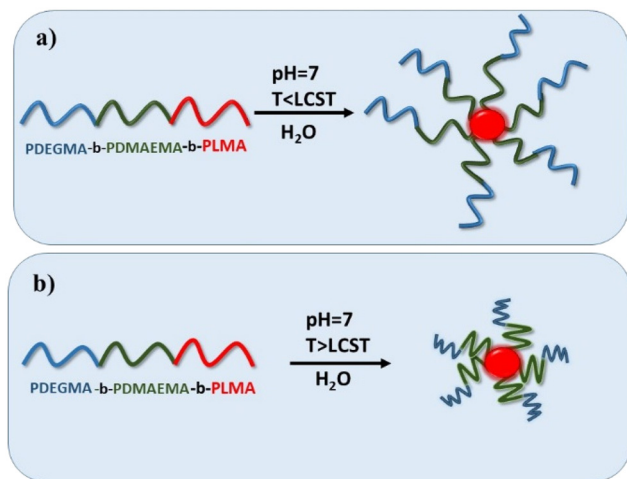
Scheme 2 Graphical representation of the self-assembly of PDEGMA-b-PDMAEMA-b-PLMA triblock terpolymer at temperatures below (a) and above (b) LCST value of PDEGMA block.

in order to determine the apparent molecular weights ($M_{w, app}$), aggregation numbers (N_{agg}) and hydrodynamic radius (R_h) of the polymeric micelles formed in aqueous solutions as a function of temperature and solution pH. The obtained results from light scattering measurements at 25 °C and 55 °C (temperature above the LCST value of the PDEGMA block) are listed in Table 2.

At pH = 7, the obtained $M_{w, app}$ values, as can be observed in Table 2, are much higher than the molecular weight of the free chains (M_w) determined by SEC for the terpolymers and the theoretical M_w calculated at 100% conversion for the quaternized terpolymers, indicating the formation of micellar nanostructures. In addition, the aggregation number (N_{agg}) is in the range from 77 to 184 at 25 °C, due to the hydrophobic PLMA block, which leads to the formation of micellar nanostructures. At 55 °C (temperature above the LCST values of PDEGMA and PDMAEMA blocks), the aggregation number is increased and specifically the formed PDEGMA$_{15}$-b-PDMAEMA$_8$-b-PLMA$_3$-3 micelles show the highest value compared to the other two triblock terpolymers due to the higher content in PDEGMA. It is worth noting that the N_{agg} values of the quaternized triblock terpolymers at both 25 °C and 55 °C are significantly lower than those of the amine-based terpolymers because of the increased solubility since the QPDMAEMA blocks bear permanent positive charges.

At 25 °C, the R_h values of the triblock terpolymers (amine and quaternized) PDEGMA$_{23}$-b-(Q)PDMAEMA$_{23}$-b-PLMA$_8$-1 and PDEGMA$_{17}$-b-(Q)PDMAEMA$_{14}$-b-PLMA$_6$-2 are higher compared to the R_h values of the PDEGMA$_{15}$-b-(Q)PDMAEMA$_8$-b-PLMA$_3$-3 terpolymer, which may lead to the conclusion that the size of the formed micelles depends on the composition of the triblock terpolymers. As the content of the hydrophobic PLMA block increases, the size of the formed micelles becomes larger. Lower R_h values are observed for the quaternized terpolymers that is attributed to the permanent positive charges of the PDMAEMA block leading to increased solubility of the terpolymers. At 55 °C, the R_h values decrease in the cases of PDEGMA$_{23}$-b-PDMAEMA$_{23}$-b-PLMA$_8$-1 and PDEGMA$_{17}$-b-PDMAEMA$_{14}$-b-PLMA$_6$-2 micelles due to the shrinkage of the formed micelle coronas as temperature increases. PDEGMA$_{15}$-b-PDMAEMA$_8$-b-PLMA$_3$-3 micelles present increased aggregation as temperature increases due to the larger amount of the thermoresponsive PDEGMA block. The PDMAEMA block is located between the hydrophobic PLMA block that occupies the core of the micelles and the PDEGMA block that, presumably, forms the outer part of the micelle corona.

Electrophoretic light scattering (ELS) measurements were carried out to determine the surface charge of the formed micelles of the triblock terpolymers. The results of the measurements are listed in Table 2. At pH = 7, the ζ-potential values are positive for all triblock terpolymers before and after the chemical modification of amine groups because of the existence of the (Q)PDMAEMA block which is partially or fully protonated at neutral solution pH.[53,59] Furthermore, for the quaternized terpolymers in which the chains of the QPDMAEMA block are positively charged permanently, the ζ-

Table 2 Light scattering and fluorescence spectroscopy results of triblock terpolymer micelles in aqueous solution at pH = 7 and at 25 °C and 55 °C

Sample	T (°C)	$M_{w, app}$ (×10⁶)[a] (g mol⁻¹)	L[b] (nm)	N_{agg}	R_h[c] (mn)	CMC[d] (×10⁻⁶) (g mL⁻¹)[58]	ζ_P[e] (mV)
PDEGMA₂₃-b-PDMAEMA₂₃-b-PLMA₈-1	25	1.7	13	168	75	2.08	+20
	55	15.2		1504	52	—	+23
PDEGMA₁₇-b-PDMAEMA₁₄-b-PLMA₆-2	25	1.15	9	164	72	1.74	+18
	55	11.8		1685	45	—	+25
PDEGMA₁₅-b-PDMAEMA₈-b-PLMA₃-3	25	0.9	6	184	58	4.29	+10
	55	21.0		4286	434	—	+4
PDEGMA₂₃-b-QPDMAEMA₂₃-b-PLMA₈-1	25	0.62	13	46	17	4.70	+27
	55	9.2		692	15	—	+41
PDEGMA₁₇-b-QPDMAEMA₁₄-b-PLMA₆-2	25	0.45	9	64	14	4.04	+24
	55	7.50		833	15	—	+40
PDEGMA₁₅-b-QPDMAEMA₈-b-PLMA₃-3	25	0.3	6	77	10	7.80	+12
	55	15.3		2550	112	—	+5

[a] Determined by SLS. [b] Calculated length of the fully extended macromolecular chain based on the total number of monomers multiplied by 0.254 nm. [c] Determined by DLS at 90° angle due to absence of angular dependence. [d] Determined by FS utilizing pyrene as the probe. [e] Determined by ELS.

potential values are significantly higher than those of the amine-based terpolymers in which the chains of the PDMAEMA block are partially protonated. Another evidence for the successful chemical modification of tertiary amine groups to quaternary amine groups is the extracted results from electrophoretic light scattering measurements. It can be observed that the surface charge values of the formed micelles undergo changes, even though the uncharged PDEGMA chains are expected to be located on their outer surface (based on the topology of the blocks, some mixing of the hydrophilic blocks may take place in the micelle corona). This fact may be attributed to the conformational alterations of the polymer chains in the formed micelles. In the cases of PDEGMA₂₃-b-QPDMAEMA₂₃-b-PLMA₈-1 and PDEGMA₁₇-b-QPDMAEMA₁₄-b-PLMA₆-2 micelles, the length of the cationic QPDMAEMA chains is longer and as a result, the positive charges of the QPDMAEMA block may be closer to the surface of the formed micelles. The ζ-potential values of these two terpolymers are higher compared to the PDEGMA₁₅-b-QPDMAEMA₈-b-PLMA₃-3 terpolymer, in which the length of the PDEGMA block is longer and thus partially hides the positive charges of the PDMAEMA block.

Effects of temperature and solution pH on the self-assembly behavior of PDEGMA-b-PDMAEMA-b-PLMA triblock terpolymers

Taking into account the nature of the blocks that constitute the triblock terpolymers and in particular the combination of the thermoresponsive PDEGMA block, the pH-responsive PDMAEMA block and the hydrophobic PLMA block in the same macromolecule makes the investigation of their properties in aqueous solutions quite interesting. The research is focused on how the alteration in one of these parameters, temperature and pH, individually or simultaneously affects the self-assembly behavior of triblock terpolymers in aqueous solutions. In order to investigate in depth the influence of temperature and pH on the self-assembly of amino-based tri-

block terpolymers in aqueous media, light scattering measurements were carried out in acidic, neutral and basic pH solutions of amino-based copolymers and measured at temperatures in the range of 25 °C–55 °C.

At pH = 3 (Fig. 2a), it can be observed that the hydrodynamic radius (R_h) of PDEGMA₂₃-b-PDMAEMA₂₃-b-PLMA₈-1 terpolymer remains constant up to 50 °C and from 50 °C to 55 °C decreases sharply (presumably aggregates decrease in size) and the scattering intensity increases as the solution temperature increases (the mass of the formed micellar nanostructures increases). At acidic solution pH, the PDMAEMA block is fully protonated, so the changes in the mass and size of the aggregates are attributed to the thermoresponsive character of the PDEGMA block. The PDEGMA₁₇-b-PDMAEMA₁₄-b-PLMA₆-2 triblock terpolymer (Fig. 2b) exhibits similar behavior, where the scattering intensity increases as the temperature increases. However, the hydrodynamic radius remains constant up to 35 °C followed by a decrease from 35 °C to 55 °C. The PDEGMA₁₇-b-PDMAEMA₁₄-b-PLMA₆-2 triblock terpolymer has a similar composition but lower molecular weight than the PDEGMA₂₃-b-PDMAEMA₂₃-b-PLMA₈-1 triblock terpolymer, so the thermoresponsive behavior of the PDEGMA block seems to affect the self-assembly process in a more intense way. Concerning the PDEGMA₁₅-b-PDMAEMA₈-b-PLMA₃-3 triblock terpolymer (Fig. 2c), it can be observed that the hydrodynamic radius presents a tendency for attaining a plateau up to 40 °C and increases from 40 °C to 55 °C. In parallel the scattering intensity remains constant up to 45 °C and increases sharply from 45 °C to 55 °C. The increase in size and mass for the polymeric micelles up to 40 °C is probably attributed to the increased content of the PDEGMA block since the solution temperature increases above the LCST value, the aggregation tendency of the formed micelles also increases.

At pH = 7, PDEGMA₂₃-b-PDMAEMA₂₃-b-PLMA₈-1 and PDEGMA₁₇-b-PDMAEMA₁₄-b-PLMA₆-2 terpolymers (Fig. 2d and e) present a similar self-assembly behavior. In particular, the hydrodynamic radius decreases as the solution temperature
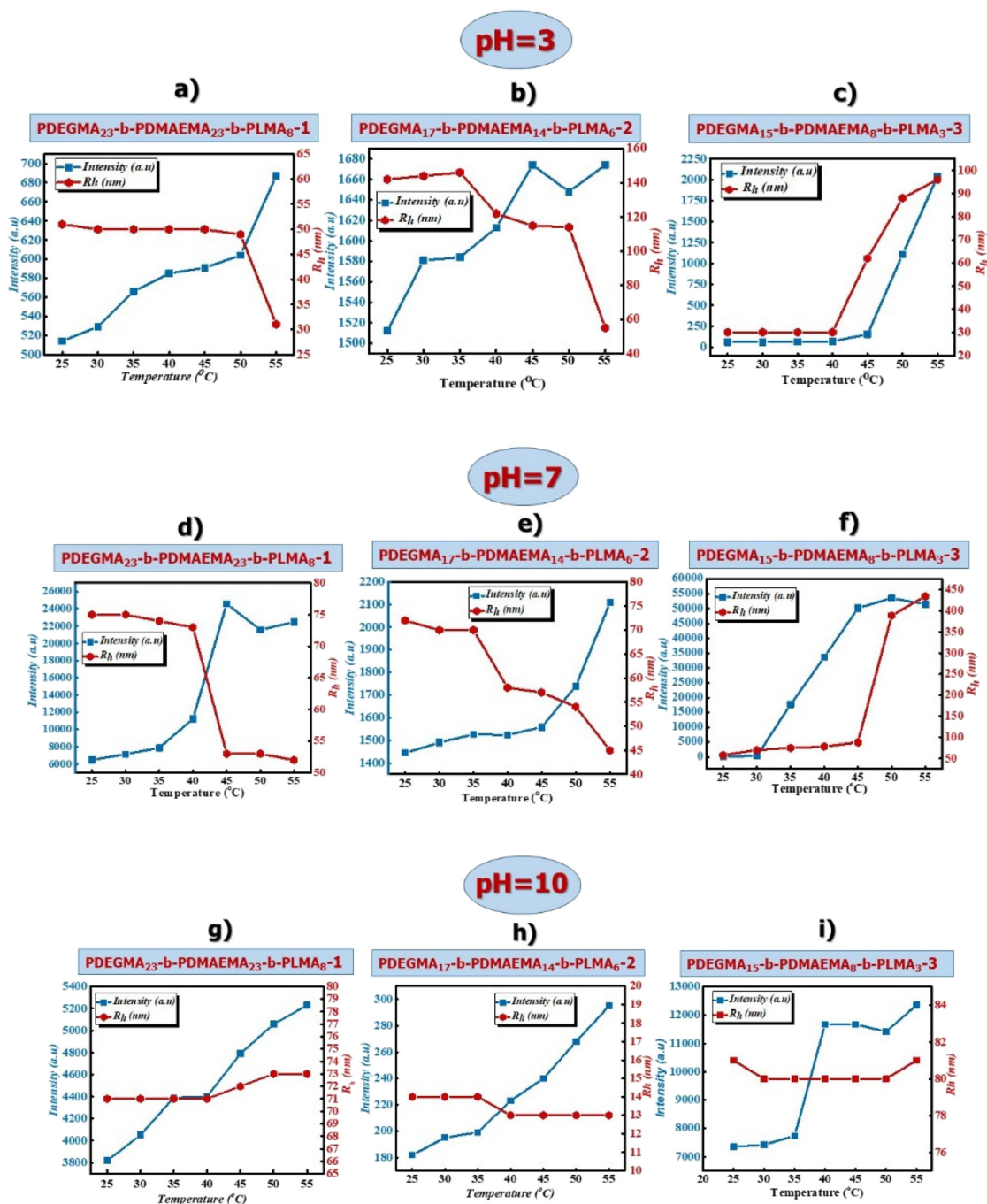
Fig. 2 Dependence of R_h and scattered light intensity on temperature for the three triblock terpolymers in aqueous media at pH = 3 (a, b, c), pH = 7 (d, e, f) and pH = 10 (g, h, i). (Measurements made at an angle of 90°.)

increases and it can be observed at temperatures above the LCST value of the PDEGMA block, which is attributed to the shrinkage of terpolymer chains as the solution temperature raises. Moreover, the scattering intensity increases at elevated temperatures, indicating an increase in the mass of the polymeric micelles (aggregation is taking place). Concerning terpolymer PDEGMA$_{15}$-b-PDMAEMA$_8$-b-PLMA$_3$-3 (Fig. 2f), the scattering intensity increases drastically from 30 °C to 35 °C and from 45 °C, a plateau can be observed and concurrently the

hydrodynamic radius of the polymeric aggregates exhibits a rapid increase from 45 °C to 55 °C. For the PDEGMA$_{15}$-b-PDMAEMA$_8$-b-PLMA$_3$-3, the response of the PDEGMA block to variations in solution temperature dictates the aggregation of the polymeric system. For all terpolymer systems, the thermo-responsive behavior of the PDMAEMA block is expected to contribute to the observed behavior at temperatures above 45 °C.

At pH = 10, for the three triblock terpolymers (Fig. 2g–i) the hydrodynamic radius values remain practically unchanged

while scattered light intensity increases with increasing temperature. At basic pH, the PDMAEMA chains are fully deprotonated, therefore the changes in the mass of the polymeric aggregates are attributed to the thermoresponsive nature of both the PDEGMA block and PDMAEMA block.

In Fig. S4† the size distributions for the three triblock terpolymers, extracted by dynamic light scattering measurements at selected temperatures (25 °C and 55 °C) and at three different solution pHs (pH 3, 7, 10), are presented.

As can be observed, monomodal size distributions are presented for nearly all terpolymers at both temperatures (25 °C and 55 °C) and at different solution pH values. However, for the PDEGMA$_{15}$-b-PDMAEMA$_8$-b-PLMA$_3$-3 triblock terpolymer (Fig. S4c†) at pH = 7 and at 25 °C there are two peaks indicating the presence of two different structures in the polymer solution. The peak with $R_h \approx 6$ nm, which is equal to the length of the extended polymer chain, (L), most probably refers to single, non-interacting polymer chains, and the peak with $R_h \approx 60$ nm is attributed to interacting polymeric chains that form micellar structures. Additionally, at 55 °C the size distributions in the majority of cases become narrower and more symmetric, indicating that the PDEGMA block, which is located in the outer part of the formed micelles, plays an important role in the self-assembly process of the triblock terpolymers.

From the results obtained by static light scattering (SLS), the R_g/R_{h0} ratio values are in the range of 0.7–0.93 for all triblock terpolymers and for the investigated stimuli (temperature and pH), which shows that the formed nanostructures obtain a spherical morphology (probably a core–shell–corona structure).

Effects of temperature and solution pH on the self-assembly behavior of PDEGMA-b-QPDMAEMA-b-PLMA quaternized triblock terpolymers

The behavior of PDEGMA-b-QPDMAEMA-b-PLMA quaternized triblock terpolymers in aqueous solutions was examined using light scattering techniques. In Fig. 3 the dependence of the scattering intensity and the hydrodynamic radius as a function of temperature for the chemically modified triblock terpolymers in aqueous media is presented.

For the PDEGMA$_{23}$-b-QPDMAEMA$_{23}$-b-PLMA$_8$-1 (Fig. 3a) cationic terpolymer, the values of the scattering intensity decrease while the values of R_h remain practically unchanged as the solution temperature increases, showing that the formed micelles decrease in mass, but their size remains unchanged with increasing solution temperature, indicating a decrease in aggregation number for the chemically modified cationic terpolymers. The values of the scattering intensity and hydrodynamic radius of the cationic PDEGMA$_{17}$-b-QPDMAEMA$_{14}$-b-PLMA$_6$-2 triblock terpolymer (Fig. 3b) remain almost invariant upon changes in temperature. This behavior may be attributed to the lower molecular weight of the cationic terpolymer resulting in the formation of a more compact micellar structure and therefore, the dimensions of the micelles were not affected noticeably by changes in the solution temperature. For the cationic terpolymer PDEGMA$_{15}$-b-QPDMAEMA$_8$-b-PLMA$_3$-3 (Fig. 3c), the values of the scattering intensity and hydrodynamic radius remain almost constant from 25 °C to 45 °C and then increase sharply up to 55 °C. The PDEGMA$_{15}$-b-QPDMAEMA$_8$-b-PLMA$_3$-3 cationic terpolymer has higher content of the PDEGMA thermoresponsive block compared to the other two cationic terpolymers, showing that at temperatures above the LCST value, the formed nanostructures increase both in size and mass. These should be clusters of micelles formed by interactions between the more hydrophobic coronas at higher temperatures.

The size distributions for the quaternized triblock terpolymers at selected temperatures are shown in Fig. S5.†

Apparently, the cationic triblock terpolymers PDEGMA$_{23}$-b-QPDMAEMA$_{23}$-b-PLMA$_8$-1 (Fig. S5a†) and PDEGMA$_{17}$-b-QPDMAEMA$_{14}$-b-PLMA$_6$-2 (Fig. S5b†) self-assemble in aqueous media into well-defined micellar nanostructures at both 25 °C and 55 °C, showing narrow and symmetric size distributions. At 25 °C, the PDEGMA$_{15}$-b-QPDMAEMA$_8$-b-PLMA$_3$-3 cationic triblock terpolymer solution (Fig. S5c†) shows a peak with $R_h \approx 10$ nm, which corresponds to micellar nanostructures (value approximately equal to the length of the extended chain, L)
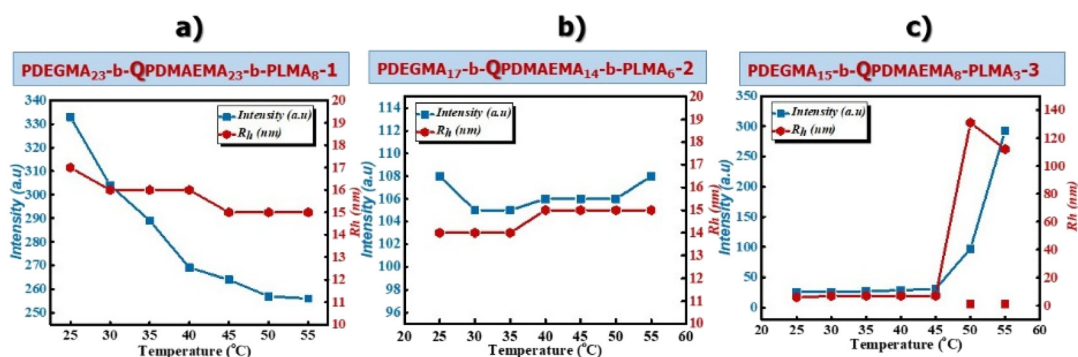

Fig. 3 Dependence of R_h and scattered light intensity on temperature for the quaternized triblock terpolymers PDEDMA$_{23}$-b-QPDMAEMA$_{23}$-b-PLMA$_8$ (a), PDEDMA$_{17}$-b-QPDMAEMA$_{14}$-b-PLMA$_6$ (b) and PDEDMA$_{15}$-b-QPDMAEMA$_8$-b-PLMA$_3$ (c), in aqueous media (measuring angle of 90°).

and a peak with $R_h \approx 112$ nm at 55 °C, which may be attributed to aggregates of micelles (clusters).

Importantly, the micelles of the chemically modified triblock terpolymers are smaller than those of the amine-based triblock terpolymers at the corresponding temperatures, which can be attributed to the better solubility of the cationic terpolymers because of the permanent positive charges on the QPDMAEMA block. The positive charges accumulate on the surface of the formed micelles resulting to the electrostatic and steric stability of the formed nanostructures.

Micelleplex formation between cationic triblock terpolymers and DNA molecules

The cationic micelles of PDEGMA-*b*-QPDMAEMA-*b*-PLMA triblock terpolymers were investigated for their ability to complex with DNA molecules. In this case complexation takes place through electrostatic interactions between the negatively charged phosphate groups of DNA molecules (P) and the positively charged ammonium groups of quaternized polymeric micelles (N). Solutions of the polymeric micelles/DNA complexes were prepared in the range of N/P = 0.5–8.0, using short length DNA ($\approx$113 bp). The cationic triblock terpolymers utilized in these studies were PDEGMA$_{23}$-*b*-QPDMAEMA$_{23}$-*b*-PLMA$_8$-1 and PDEGMA$_{17}$-*b*-QPDMAEMA$_{14}$-*b*-PLMA$_6$-2 and their molecular characteristics are listed in Table 1.

UV-vis spectroscopy measurements were performed to confirm the successful formation of PDEGMA-*b*-QPDMAEMA-*b*-PLMA/DNA micelleplexes. The complexation capability of cationic polymers with DNA molecules is usually examined by performing UV–vis measurements as the absorption of DNA molecules in this spectral region provides considerable information on possible variations in the conformation state of nucleic acid double helix originating from the interactions between the DNA molecules and the cationic polymers. According to the literature,[60] before complexation, naked DNA molecules display a characteristic absorption peak at 260 nm. In our systems, this characteristic peak decreases in intensity

while the nucleic acid interacts with the positively charged terpolymers forming micelleplexes and eventually disappears as the N/P ratio increases, whereas simultaneously a new characteristic peak becomes visible at 225 nm. This absorption peak is attributed to the complexed DNA molecules, as the triblock terpolymers examined present no absorption in the UV–vis region as verified by UV–vis spectroscopy measurements.

In Fig. 4, the characteristic peak of DNA molecules at 260 nm before complexation with the cationic micelles can be observed. After the complexation between DNA molecules and cationic micelles, the peak at 260 nm decreases and eventually disappears while a new peak appears at around 225 nm, which corresponds to the complexed DNA molecules. For the PDEGMA$_{23}$-*b*-QPDMAEMA$_{23}$-*b*-PLMA$_8$-1/DNA (Fig. 4a) and PDEGMA$_{17}$-*b*-QPDMAEMA$_{14}$-*b*-PLMA$_6$-2/DNA (Fig. 4b) complexes, it can be observed that for N/P ratios in the range from 0.5 to 2, there are two peaks (at 225 nm and 260 nm) which may be attributed to the existence of complexed and non-complexed DNA molecules in the solution. The peak at 260 nm disappears as the concentration of the cationic polymer increases and only the peak at 225 nm can be noticed, which means that the majority of DNA molecules in the solution take part in the formation of the micelleplexes. Increasing the concentration of cationic polymers in the solution leads to an increase in positive charges, which neutralize the negative charges of the DNA molecules. However, it can be observed that the peak attributed to non-complexed DNA molecules at 260 nm is more intense in the case of PDEGMA$_{17}$-*b*-QPDMAEMA$_{14}$-*b*-PLMA$_6$-2/DNA micelleplexes, which means that the DNA molecules interact in a more potent way with the cationic PDEGMA$_{23}$-*b*-QPDMAEMA$_{23}$-*b*-PLMA$_8$-1 micelles due to the longer QPDMAEMA block.

Ethidium bromide (EtBr) is a vastly utilized fluorescent probe for evaluating the binding affinity between cationic polymers and DNA molecules since it is able to interact with nucleic acid molecules by intercalation into the base pairs of the DNA helix.[61,62] Particularly, the formation of polyplexes
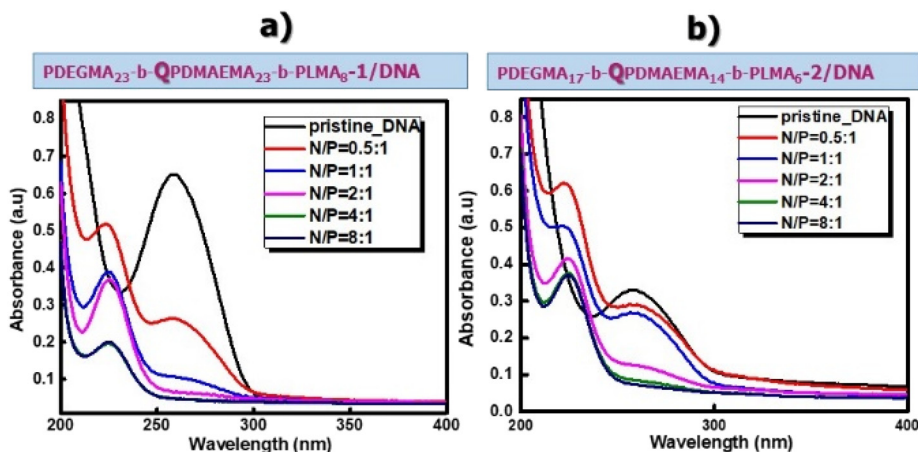

Fig. 4 UV–vis spectra of naked DNA and PDEGMA$_{23}$-*b*-QPDMAEMA$_{23}$-*b*-PLMA$_8$-1/DNA (a) and PDEGMA$_{17}$-*b*-QPDMAEMA$_{14}$-*b*-PLMA$_6$-2/DNA (b) micelleplexes at N/P ratios in the range of 0.5–0.8.
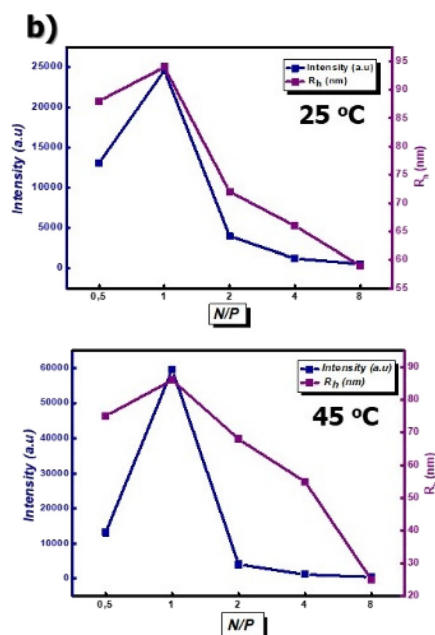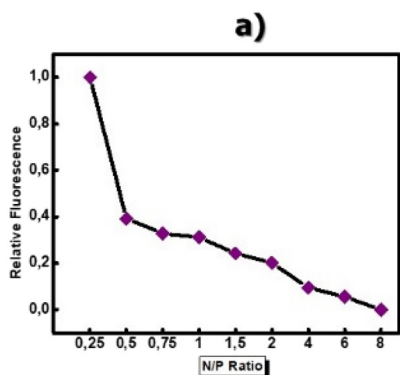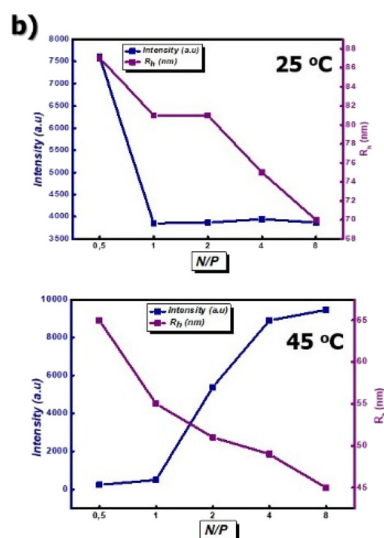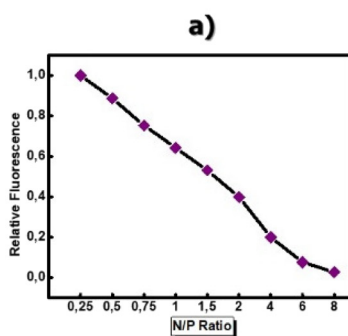
Fig. 5 (a) Ethidium bromide fluorescence quenching for PDEGMA$_{23}$-*b*-QPDMAEMA$_{23}$-*b*-PLMA$_8$-1/DNA and PDEGMA$_{17}$-*b*-QPDMAEMA$_{14}$-*b*-PLMA$_6$-2/DNA micelleplexes. (b) Alterations of scattered intensity and hydrodynamic radius (R_h) with N/P ratio for PDEGMA$_{23}$-*b*-QPDMAEMA$_{23}$-*b*-PLMA$_8$-1/DNA and PDEGMA$_{17}$-*b*-QPDMAEMA$_{14}$-*b*-PLMA$_6$-2/DNA at 25 °C and 45 °C and at an angle of 90°.

was investigated by monitoring the decrease in the relative fluorescence intensity as ethidium bromide molecules were displaced from the double-stranded DNA by the cationic polymer in a titration assay. In Fig. 5, the curves of EtBr relative fluorescence intensity for PDEGMA$_{23}$-*b*-QPDMAEMA$_{23}$-*b*-PLMA$_8$-1 and PDEGMA$_{17}$-*b*-QPDMAEMA$_{14}$-*b*-PLMA$_6$-2 (Fig. 5a) cationic terpolymer micelles with DNA molecules as a function of N/P ratio are presented.

For both cases, as the concentration of the cationic terpolymer in the solution increases, the fluorescence intensity of

EtBr decreases. This considerable quenching of the fluorescence intensity is related to the displacement of intercalated EtBr molecules from the DNA double helix indicating an intense complexation capability of the examined cationic terpolymers. In particular, the decrease is steeper in the case of PDEGMA$_{23}$-*b*-QPDMAEMA$_{23}$-*b*-PLMA$_8$-1/DNA micelleplexes, which indicates faster and better/stronger complexation, which is also verified by the results from the UV-Vis spectroscopy measurements reported above. The PDEGMA$_{23}$-*b*-QPDMAEMA$_{23}$-*b*-PLMA$_8$-1 cationic terpolymer seems to inter-

act strongly with nucleic acid molecules that may be attributed to the higher content of the QPDMAEMA block. From these observations, it was found that the cationic triblock terpolymers are able to interact with DNA molecules and it should be pointed out that the molecular weight and composition of cationic terpolymers play a significant role in their ability to form micelleplexes with DNA molecules.

In Fig. 5b, the representative plots of the scattering intensity and hydrodynamic radius for the micelleplexes at selected temperatures (25 °C and 45 °C) in the whole N/P range are depicted. It can be seen that the PDEGMA$_{23}$-b-QPDMAEMA$_{23}$-b-PLMA$_8$-1/DNA micelleplexes present higher intensity than the PDEGMA$_{17}$-b-QPDMAEMA$_{14}$-b-PLMA$_6$-2/DNA micelleplexes at both 25 °C and 45 °C as well as in the whole range of N/P ratios, which indicates the existence of larger in mass polymer–DNA nanoparticles.

The scattering intensity of PDEGMA$_{23}$-b-QPDMAEMA$_{23}$-b-PLMA$_8$-1/DNA complexes at 25 °C almost doubles from N/P = 0.5 to N/P = 1, a region where the negatively charged phosphate groups of DNA molecules are in excess. The scattering intensity decreases, from N/P = 1 to N/P = 8 ratios, where the quaternized amino groups of the QPDMAEMA block are equal or in excess to the phosphate groups of the DNA molecules. At 45 °C, the scattering intensity of PDEGMA$_{23}$-b-QPDMAEMA$_{23}$-b-PLMA$_8$-1/DNA complexes increases nearly sixfold from N/P = 0.5 to N/P = 1 and then sharply decreases from N/P = 1 to N/P = 8. The different behavior of the formed micelleplexes is probably attributed to the thermoresponsive behavior of the cationic micelles maintained even after their complexation with the DNA molecules. The scattering intensity of PDEGMA$_{17}$-b-QPDMAEMA$_{14}$-b-PLMA$_6$-2/DNA micelleplexes at 25 °C decreases sharply from N/P = 0.5 to N/P = 1 and then from N/P = 1 to N/P = 8 without showing significant changes. In contrast, at 45 °C, the scattering intensity increases in the whole range of N/P ratios. The hydrodynamic radii of the micelles formed by PDEGMA$_{23}$-b-QPDMAEMA$_{23}$-b-PLMA$_8$-1 and PDEGMA$_{17}$-b-QPDMAEMA$_{14}$-b-PLMA$_6$-2 terpolymers before

complexing with DNA molecules are R_h = 17 nm and R_h = 14 nm, respectively. After complexation with DNA molecules, the R_h values increase, which indicates the successful formation of micelleplexes. However, the R_h values decrease as the N/P ratio increases, showing that the excess of quaternized amine groups in the mixed polymer–DNA solutions promotes the formation of more compact micelleplexes.

Fig. S6† demonstrates the size distributions obtained by DLS experiments for the PDEGMA$_{23}$-b-QPDMAEMA$_{23}$-b-PLMA$_8$-1/DNA and PDEGMA$_{17}$-b-QPDMAEMA$_{14}$-b-PLMA$_6$-2/DNA micelleplexes at various N/P ratios and at selected temperatures. The micelleplexes formed present monomodal size distributions in all cases. However, it can be observed that the changes in solution temperature affect the size distributions of PDEGMA$_{23}$-b-QPDMAEMA$_{23}$-b-PLMA$_8$-1/DNA micelleplexes (Fig. S6a†) in a more prominent way compared to PDEGMA$_{17}$-b-QPDMAEMA$_{14}$-b-PLMA$_6$-2/DNA (Fig. S6b†) micelleplexes indicating that the molecular characteristics of the cationic terpolymers and the changes in solution temperature play an important role in the formation and structure of micelleplexes. The increased amount of PDEGMA and QPDMAEMA blocks in PDEGMA$_{23}$-b-QPDMAEMA$_{23}$-b-PLMA$_8$-1/DNA micelleplexes may be the reason for this difference in behavior.

The values of zeta potential extracted by ELS measurements for the micelleplexes in the whole range of N/P ratio studies are depicted in Fig. 6. The measurements are conducted at both 25 °C and 45 °C, to examine the surface charge of the formed micelleplexes at the mentioned temperatures. At N/P = 0.5, for both PDEGMA$_{23}$-b-QPDMAEMA$_{23}$-b-PLMA$_8$-1/DNA (Fig. 6a) and PDEGMA$_{17}$-b-QPDMAEMA$_{14}$-b-PLMA$_6$-2/DNA (Fig. 6b), the zeta potential values are negative. This may be explained by the fact that at this N/P ratio the negatively charged phosphate groups of the DNA molecules are in excess and as a result there are DNA molecules that have not been complexed/interacted with positively charged amine groups or DNA molecules populate the surface of micelleplexes. At N/P = 1, where the negatively charged phosphate groups of the DNA
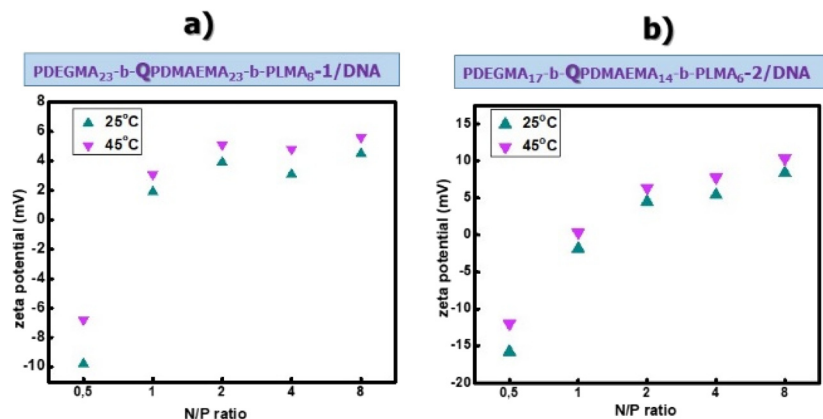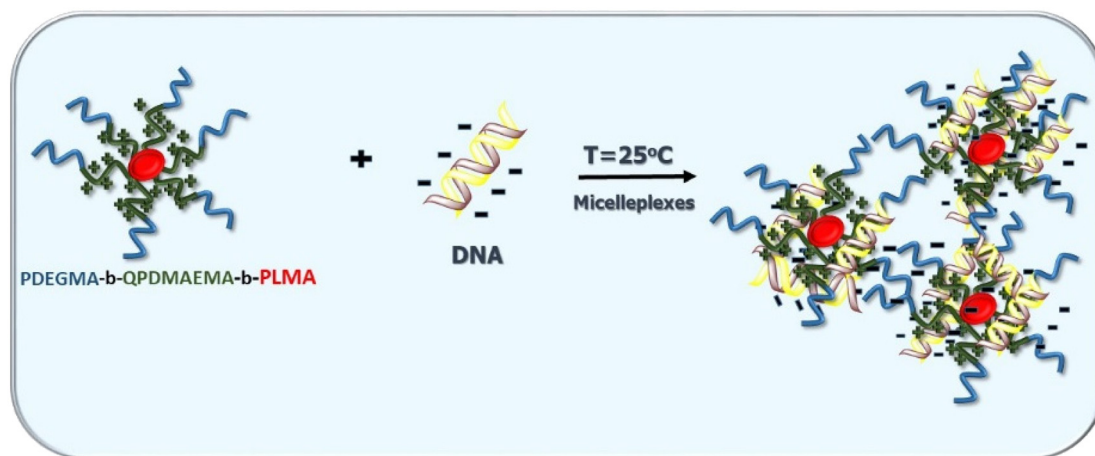

Fig. 6 Zeta-potential values *vs.* N/P ratios for PDEGMA$_{23}$-b-QPDMAEMA$_{23}$-b-PLMA$_8$-1/DNA (a) and PDEGMA$_{17}$-b-QPDMAEMA$_{14}$-b-PLMA$_6$-2/DNA (b) micelleplexes at 25 °C and 45 °C.

Scheme 3 Schematic representation of PDEGMA-*b*-QPDMAEMA-*b*-PLMA/DNA micelleplexes at 25 °C.

molecules were expected to be neutralized by the positively charged amine groups of the cationic QPDMAEMA block, the zeta potential is almost zero. At N/P > 1, where the cationic terpolymers are in excess, a plateau is attained where the zeta potential shows positive values and displays minor changes with N/P. This signifies that most of the negatively charged phosphate groups have been complexed with the positively charged amine groups and as a result the cationic terpolymer systems present increased efficiency for micelleplex formation.

From the results discussed so far, it can be deduced that the thermoresponsive cationic terpolymers are capable of complexing with DNA molecules *via* electrostatic interactions. Scheme 3 is an illustration of nucleic acid binding with the temperature-responsive cationic triblock terpolymers towards the formation of micelleplexes.

Conclusions

Thermoresponsive and pH-responsive PDEGMA-*b*-PDMAEMA-*b*-PLMA triblock terpolymers having various compositions of the blocks and different molecular weights were successfully synthesized utilizing RAFT polymerization techniques. The quaternization reaction of the PDMAEMA block using CH_3I as the quaternizing agent converted the linear triblock terpolymers into strong cationic polyelectrolytes giving PDEGMA-*b*-QPDMAEMA-*b*-PLMA terpolymers. The results obtained by molecular characterization of all synthesized terpolymers presented evidence of well-defined terpolymers with controlled compositions and molecular weights.

Studies on the self-assembly behavior of these triblock terpolymers in aqueous media showed that they form spherical micelles where the PDMAEMA block is located between the hydrophobic PLMA block that occupies the core of the micelles and the PDEGMA block that forms the outer surface of the micellar shell, as proven by light scattering experiments. The CMC of the formed micelles depends on the PLMA hydro-

phobic content and the charge of the triblock terpolymers. The variations in temperature and pH values seem to affect the self-assembly behavior of the formed micelles. The chemical composition of these triblock terpolymers and their positive charge make them attractive nanocarriers for gene delivery. The thermoresponsive and cationic micelles of PDEGMA-*b*-QPDMAEMA-*b*-PLMA triblock terpolymers were found to interact with DNA molecules *via* electrostatic interactions forming micelleplexes, with good colloidal stability. The formation of micelleplexes is confirmed by UV–vis measurements, as well as FS measurements of ethidium bromide quenching. Particularly, the results obtained by physiochemical characterization reveal a strong complexation between cationic $PDEGMA_{23}$-*b*-$QPDMAEMA_{23}$-*b*-$PLMA_8$-1 micelles, with a higher content of the QPDMAEMA block, and DNA molecules. In contrast, the cationic $PDEGMA_{17}$-*b*-$QPDMAEMA_{14}$-*b*-$PLMA_6$-2 micelles with a lower QPDMAEMA content present lower effectiveness in displacing EtBr molecules and less efficient interaction capability with nucleic acid macromolecules. Moreover, the physiochemical results obtained by light scattering experiments (DLS and ELS) at 25 °C and after raising the solution temperature to 45 °C revealed that the composition of block terpolymers, the N/P ratio, and the increase of temperature above the LCST value of PDEGMA strongly affected the surface charge and the overall dimensions of the resulting micelleplexes through secondary temperature triggered aggregation. In conclusion, the physiochemical characterization results provide important information on the parameters affecting cationic terpolymer/DNA interactions and ultimately demonstrate the potential of PDEGMA-*b*-QPDMAEMA-*b*-PLMA cationic micelles to be utilized as temperature-responsive non-viral gene vectors.

Conflicts of interest

The authors have no competing interests to declare.

References

1 Q. Tian, C. Fei, H. Yin and Y. Feng, *Prog. Polym. Sci.*, 2019, **89**, 108–132.

2 M.-H. Li and P. Keller, *Soft Matter*, 2009, **5**, 927–937.

3 S. Ganta, H. Devalapally, A. Shahiwala and M. Amiji, *J. Controlled Release*, 2008, **126**, 187–204.

4 E. Cabane, X. Zhang, K. Langowska, C. G. Palivan and W. Meier, *Biointerphases*, 2012, **7**, 1–27.

5 A. W. York, S. E. Kirkland and C. L. McCormick, *Adv. Drug Delivery Rev.*, 2008, **60**, 1018–1036.

6 D. Schmaljohann, *Adv. Drug Delivery Rev.*, 2006, **58**, 1655–1670.

7 F. D. Jochum and P. Theato, *Chem. Soc. Rev.*, 2013, **42**, 7468–7483.

8 J.-F. Gohy and Y. Zhao, *Chem. Soc. Rev.*, 2013, **42**, 7117–7129.

9 G. Kocak, C. Tuncer and V. Bütün, *Polym. Chem.*, 2017, **8**, 144–176.

10 J. E. Laaser, Y. Jiang, D. Sprouse, T. M. Reineke and T. P. Lodge, *Macromolecules*, 2015, **48**, 2677–2685.

11 M. A. Ward and T. K. Georgiou, *Polymers*, 2011, **3**, 1215–1242.

12 D. Roy, W. L. Brooks and B. S. Sumerlin, *Chem. Soc. Rev.*, 2013, **42**, 7214–7243.

13 Y. Kotsuchibashi, M. Ebara, T. Aoyagi and R. Narain, *Polymers*, 2016, **8**, 380.

14 N. Shimada, H. Ino, K. Maie, M. Nakayama, A. Kano and A. Maruyama, *Biomacromolecules*, 2011, **12**, 3418–3422.

15 M. Nakayama, J. Akimoto and T. Okano, *J. Drug Targeting*, 2014, **22**, 584–599.

16 I. Dimitrov, B. Trzebicka, A. H. Müller, A. Dworak and C. B. Tsvetanov, *Prog. Polym. Sci.*, 2007, **32**, 1275–1343.

17 Y. Li, J. Gao, C. Zhang, Z. Cao, D. Cheng, J. Liu and X. Shuai, *Polymeric gene delivery systems,* Springer, 2017, vol. 375, pp. 167–215.

18 A. Rösler, G. W. Vandermeulen and H.-A. Klok, *Adv. Drug Delivery Rev.*, 2012, **64**, 270–279.

19 V. P. Torchilin, *Pharm. Res.*, 2007, **24**, 1–16.

20 T. G. Park, J. H. Jeong and S. W. Kim, *Adv. Drug Delivery Rev.*, 2006, **58**, 467–486.

21 J. H. Jeong, S. W. Kim and T. G. Park, *Prog. Polym. Sci.*, 2007, **32**, 1239–1274.

22 L. Klouda and A. G. Mikos, *Eur. J. Pharm. Biopharm.*, 2008, **68**, 34–45.

23 C. Pietsch, U. S. Schubert and R. Hoogenboom, *Chem. Commun.*, 2011, **57**, 8750–8765.

24 J. F. Lutz and A. Hoth, *Macromolecules*, 2006, **39**, 893–896.

25 K. Sun, M. Xu, K. Zhou, H. Nie, J. Quan and L. Zhu, *Mater. Sci. Eng., C*, 2016, **68**, 172–176.

26 S. Dai, P. Ravi and K. C. Tam, *Soft Matter*, 2008, **4**, 435–449.

27 C. Donini, D. Robinson, P. Colombo, F. Giordano and N. Peppas, *Int. J. Pharm.*, 2002, **245**, 83–91.

28 T. R. Kyriakides, C. Y. Cheung, N. Murthy, P. Bornstein, P. S. Stayton and A. S. Hoffman, *J. Controlled Release*, 2002, **78**, 295–303.

29 C. De las Heras Alarcón, S. Pennadam and C. Alexander, *Chem. Soc. Rev.*, 2005, **34**, 276–285.

30 F. A. Plamper, M. Ballauff and A. H. Müller, *J. Am. Chem. Soc.*, 2007, **129**, 14538–14539.

31 S. I. Yamamoto, J. Pietrasikand and K. Matyjaszewski, *Macromolecules*, 2008, **41**, 7013–7020.

32 K. Miyata, M. Oba, M. R. Kano, S. Fukushima, Y. Vachutinsky, M. Han, H. Koyama, K. Miyazono, N. Nishiyama and K. Kataoka, *Pharm. Res.*, 2008, **25**, 2924–2936.

33 S. Cho, C. Dang, X. Wang, R. Ragan and Y. Kwon, *Biomater. Sci.*, 2015, **3**, 1124–1133.

34 M. A. Mintzer and E. E. Simanek, *Chem. Rev.*, 2009, **109**, 259–302.

35 S. Agarwal, Y. Zhang, S. Maji and A. Greiner, *Mater. Today*, 2012, **15**, 388–393.

36 A. Pathak, S. Patnaik and K. C. Gupta, *Biotechnol. J.*, 2009, **4**, 1559–1572.

37 G. Navarro, J. Pan and V. P. Torchilin, *Mol. Pharm.*, 2015, **12**, 301–313.

38 H. Yin, R. L. Kanasty, A. A. Eltoukhy, A. J. Vegas, J. R. Dorkin and D. G. Anderson, *Nat. Rev. Genet.*, 2014, **15**, 541–555.

39 N. Nishiyama, Y. Matsumura and K. Kataoka, *Cancer Sci.*, 2016, **107**, 867–874.

40 H. Cabral, K. Miyata, K. Osada and K. Kataoka, *Chem. Rev.*, 2018, **118**, 6844–6892.

41 C. T. de Ilarduya, Y. Sun and N. Düzgünes, *Eur. J. Pharm. Sci.*, 2010, **40**, 159–170.

42 X. X. Zhang, T. J. McIntosh and M. W. Grinstaff, *Biochimie*, 2012, **94**, 42–58.

43 M. Y. Marzbali and A. Y. Khosroushahi, *Cancer Chemother. Pharmacol.*, 2017, **79**, 637–649.

44 D. B. Bitoque, S. Simão, A. V. Oliveira, S. Machado, M. R. Duran, E. Lopes, A. M. R. da Costa and G. A. Silva, *J. Tissue Eng. Regener. Med.*, 2017, **11**, 265–275.

45 B. Mahltig, P. Müller-Buschbaum, M. Wolkenhauer, O. Wunnicke, S. Wiegand, J. F. Gohy, R. Jérôme and M. Stamm, *J. Colloid Interface Sci.*, 2001, **242**, 36–43.

46 M. Allmeroth, D. Moderegger, D. Gündel, K. Koynov, H.-G. Buchholz, K. Mohr, F. Rösch, R. Zentel and O. Thews, *Biomacromolecules*, 2013, **14**, 3091–3310.

47 M. Demetriou and T. Krasia-Christoforou, *J. Polym. Sci., Part A: Polym. Chem.*, 2008, **46**, 5442–5451.

48 G. Moad, *Polym. Chem.*, 2017, **8**, 177–219.

49 N. P. Truong, M. R. Whittaker, A. Anastasaki, D. M. Haddleton, J. F. Quinn and T. P. Davis, *Polym. Chem.*, 2016, **7**, 430–440.

50 Y. Qianqian and Z. Puyu, *Adv. Mater.*, 2013, **668**, 145–148.

51 R. A. Cordeiro, N. Rocha, J. P. Mendes, K. Matyjaszewski, T. Guliashvili, A. C. Serra and J. F. Coelho, *Polym. Chem.*, 2013, **4**, 3088–3097.

52 A. Skandalis and S. Pispas, *J. Polym. Sci., Part A: Polym. Chem.*, 2017, **55**, 155–163.

53 S. Antoun and J. F. Gohy, *Polymer*, 2001, **42**, 3641–3648.

54 N. B. Colthup, S. E. Wiberley and L. H. Daly, *Introduction to Infrared and Raman Spectroscopy,* Academic Press, New York, 1975, vol. 11, p. 324.

55 J.-F. Gohy, Block Copolymer Micelles, *Adv. Polym. Sci.*, 2005, **190**, 65–136.

56 Y. Mai and A. Eisenberg, Self-assembly of block copolymers, *Chem. Soc. Rev.*, 2012, **41**, 5969–5985.

57 D. Selianitis and S. Pispas, *J. Polym. Sci.*, 2020, **58**, 1867–1880.

58 F. M. Winnik, H. Ringsdorf and J. Venzmer, *Langmuir*, 1991, **7**, 905–911.

59 J. E. Laaser, Y. Jiang, D. Sprouse, T. M. Reineke and T. P. Lodge, *Macromolecules*, 2015, **48**, 2677–2685.

60 D. Dey, S. Kumar, R. Banerjee, S. Maiti and D. Dhara, *J. Phys. Chem. B*, 2014, **118**, 7012–7025.

61 E. Haladjova, G. Mountrichas, S. Pispas and S. Rangelov, *J. Phys. Chem. B*, 2016, **120**, 2586–2595.

62 A. J. Geall and I. S. Blagbrough, *J. Pharm. Biomed. Anal.*, 2000, **22**, 849–848.